Cell Reports
Methods

Report

Modulation of neuronal activity in cortical organoids with bioelectronic delivery of ions and neurotransmitters

Graphical abstract

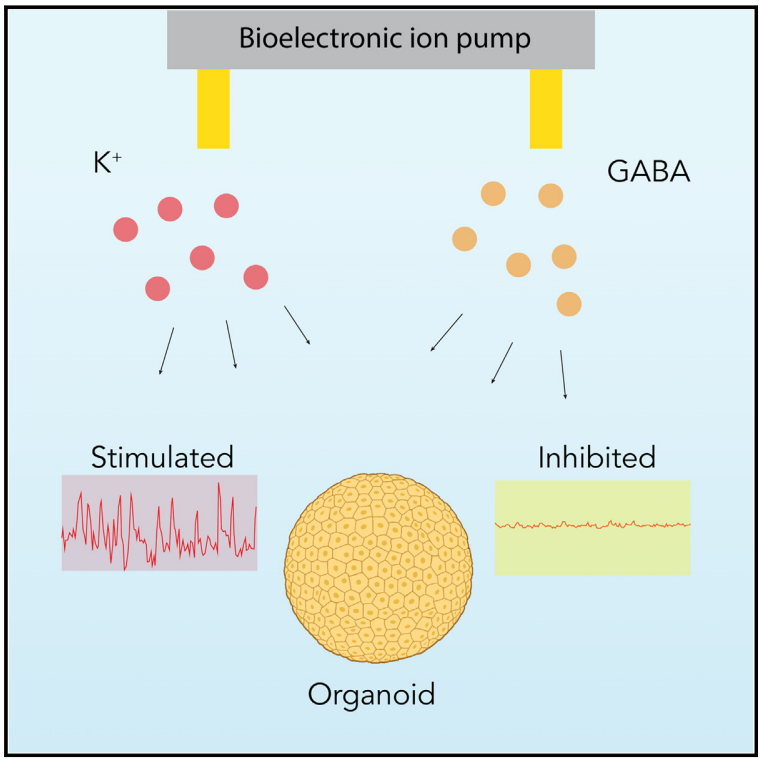

Authors

Yunjeong Park, Sebastian Hernandez, Cristian O. Hernandez, ..., Mircea Teodorescu, Mohammed A. Mostajo-Radji, Marco Rolandi

Correspondence

mteodore@ucsc.edu (M.T.), mmostajo@ucsc.edu (M.A.M.-R.), mrolandi@ucsc.edu (M.R.)

In brief

Park et al. utilize bioelectronic ion pumps to modulate neuronal activity in cortical organoids, demonstrating rapid, reversible control through targeted K^+ and GABA delivery. This approach can facilitate studies on circuit maturation and plasticity.

Highlights

- Bioelectronic ion pumps can enable precise control of cortical organoid activity
- Potassium ions and γ-aminobutyric acid are used to modulate neuronal activity
- Simultaneous network activity monitoring is possible with our approach
- Provides a proof of concept for advanced neurodevelopmental disease research

Park et al., 2024, Cell Reports Methods *4*, 100686
January 22, 2024
https://doi.org/10.1016/j.crmeth.2023.100686

CellPress

Cell Reports Methods

CellPress
OPEN ACCESS

Report

Modulation of neuronal activity in cortical organoids with bioelectronic delivery of ions and neurotransmitters

Yunjeong Park,[1,8] Sebastian Hernandez,[1,2,3,4,8] Cristian O. Hernandez,[1] Hunter E. Schweiger,[2,3,5] Houpu Li,[1] Kateryna Voitiuk,[2,6] Harika Dechiraju,[1] Nico Hawthorne,[1,2] Elana M. Muzzy,[1] John A. Selberg,[1] Frederika N. Sullivan,[2] Roberto Urcuyo,[4] Sofie R. Salama,[2,5,7] Elham Aslankoohi,[1] Heather J. Knight,[1,5] Mircea Teodorescu,[1,2,7,*] Mohammed A. Mostajo-Radji,[2,3,7,*] and Marco Rolandi[1,2,7,9,*]

[1]Department of Electrical and Computer Engineering, University of California, Santa Cruz, Santa Cruz, CA 95064, USA
[2]Genomics Institute, University of California, Santa Cruz, Santa Cruz, CA 95060, USA
[3]Live Cell Biotechnology Discovery Lab, University of California, Santa Cruz, Santa Cruz, CA 95060, USA
[4]Centro de Electroquímica y Energía Química (CELEQ), Universidad de Costa Rica, San José 11501 2060, Costa Rica
[5]Department of Molecular, Cellular and Developmental Biology, University of California, Santa Cruz, Santa Cruz, CA 95060, USA
[6]Department of Biomolecular Engineering, University of California, Santa Cruz, Santa Cruz, CA 95060, USA
[7]Institute for the Biology of Stem Cells, University of California, Santa Cruz, Santa Cruz, CA 95060, USA
[8]These authors contributed equally
[9]Lead contact
*Correspondence: mteodore@ucsc.edu (M.T.), mmostajo@ucsc.edu (M.A.M.-R.), mrolandi@ucsc.edu (M.R.)
https://doi.org/10.1016/j.crmeth.2023.100686

MOTIVATION Cortical organoids offer a promising avenue for exploring brain circuitry formation, but their potential is restrained by limited techniques for precise, temporally controlled modulation of neuronal activity. To overcome this challenge, we demonstrate bioelectronic ion pumps manipulating neuronal activity in cortical organoids through the targeted delivery of ions and neurotransmitters. By effectively modulating neuronal activity in brain organoids using potassium ions (K^+) and γ-aminobutyric acid (GABA), we demonstrate the possibility for more controlled studies on circuit maturation and plasticity.

SUMMARY

Precise modulation of brain activity is fundamental for the proper establishment and maturation of the cerebral cortex. To this end, cortical organoids are promising tools to study circuit formation and the underpinnings of neurodevelopmental disease. However, the ability to manipulate neuronal activity with high temporal resolution in brain organoids remains limited. To overcome this challenge, we introduce a bioelectronic approach to control cortical organoid activity with the selective delivery of ions and neurotransmitters. Using this approach, we sequentially increased and decreased neuronal activity in brain organoids with the bioelectronic delivery of potassium ions (K^+) and γ-aminobutyric acid (GABA), respectively, while simultaneously monitoring network activity. This works highlights bioelectronic ion pumps as tools for high-resolution temporal control of brain organoid activity toward precise pharmacological studies that can improve our understanding of neuronal function.

INTRODUCTION

Pluripotent stem cell-derived cortical organoids are valuable tools to study brain development, evolution, and disease.[1,2] Several efforts have tried to understand the emergence, development, and maturation of circuit formation in these microphysiological systems.[3–6] Moreover, circuit activity manipulation by either grafting of defined cell types[7,8] or treatment with small molecules[9,10] has shed new light on the molecular and cellular mechanisms of neurodevelopmental disorders. During development, neuronal activity plays a key role in cortical circuit establishment and maturation.[11–13] For example, neuronal activity modulation controls several processes, including fate acquisition and neuronal migration.[14–16] Similarly, other molecules, including neurotransmitters, regulate the proliferation of radial glia cells and control the migration of interneurons to the cerebral cortex.[17–21] Despite the important roles of ions and neurotransmitters in cortical development, current organoid models lack the temporal resolution to study subtle changes in the concentrations of these ions and molecules in discrete processes.

Scientists either use cell lines mutated for the receptors of interest[8] or perform bath applications of the desired ions and molecules.[22,23] To address these challenges, bioelectronic electrophoretic pumps deliver ions and charged molecules with high spatiotemporal control. They do so by driving charged ions using a potential difference across two electrodes, one placed in a reservoir with a solution containing the ion of interest and the other in the target. To ensure that only the desired ions are delivered from the reservoir to the target, ion pumps typically include an ion-selective membrane that only allows through ions and small molecules of the desired charge.[24–26] Bioelectronic ion pumps offer distinct advantages, including hydrogel-based selectivity toward specific ions, reduced invasiveness, and the ability to perform continuous and automated ion delivery.[27–29] Moreover, the development of multi-ion pumps can allow the simultaneous or sequential control of several processes.[30,31] Previous work has demonstrated the efficacy of these pumps in *in vivo* models of inflammation,[32] wound healing,[33] and epilepsy,[34] as well as the delivery of potassium ions to *in vitro* 2D models to actuate and control biological processes.[24] However, their applications to organoids and other *in vitro* 3D systems remain largely unexplored. Here, we demonstrate the modulation of neuronal activity in organoids through the spatiotemporal delivery of K^+ ions and γ-aminobutyric acid (GABA) using bioelectronic ion pumps (Figure 1).

RESULTS

Bioelectronic delivery of K^+ and GABA

Bioelectronic ion pumps have delivered ions and charged molecules to many *in vivo* and *in vitro* 2D models.[24,30] However, their application in organoids and other 3D *in vitro* systems has remained largely uncharted. To extend this technology, we adapted a specialized bioelectronic ion pump intended for delivery within 3D organoid models (Figure 1A). This ion pump delivers GABA and K^+ ions, either individually or concurrently, to a target solution containing mouse cortical organoids. As both GABA, a neurotransmitter, and K^+, a modulator of neural excitability, play vital roles in neural activity,[35,36] their delivery offers the opportunity to observe the combined effects of these charged molecules on intracellular calcium dynamics, a reliable marker of neural activity (Figure 1A). The bioelectronic pump contains four reservoirs, two of which hold 1 M KCl (left) and 100 mM GABA solutions (right) and the respective working electrodes (WEs), along with a reservoir that hosts the reference electrode (Figure 1B). An additional reservoir, not depicted, can be used as additional reference electrode (Figure S1). With a potential difference (V_{K+} for K^+ delivery and V_{GABA} for GABA delivery) between one of the WEs and the reference electrode (RE), the pump delivers K^+ and GABA from the reservoirs to the target (Figure 1B). In the K^+ delivery system, V_{K+} prompts the WE to attract the Cl^- ion part of KCl.[24,37] These ions undergo oxidation upon reaching the Ag surface, resulting in the formation of AgCl (Figure 1C). The electric field then drives the resulting K^+ ions from the WE-containing reservoir into the target through the capillary (Figure 1C). V_{K+} could drive physiological cations, such as Na^+ or Ca^{2+}, to move back into the spare chamber containing the RE.[24,30] For GABA delivery, adjusting the pH of the solution to 4 with HCl enables protonation of the GABA molecules, leading to the formation of positively charged GABA cations (Figure 1D).[34] These cations move through the anionic-hydrogel-filled capillary under the influence of an electric field.[38] The V_{GABA} between the WE and the RE attracts Cl^- ions to the Ag surface of the WE, producing AgCl in a process similar to K^+'s process[24,37] (Figures 1D and S1). After K^+ and GABA are delivered to the target solution, they eventually reach the organoids via diffusion that creates a concentration gradient in the target, with the highest concentration at the delivery site and approximately a 5-fold dilution approximately 400 mm away from the delivery site (Figure S2). To facilitate the integration of the ion pump with *in vitro* cultures, we designed a 3D-printed adapter (Figure 1E). This adapter stabilizes the ion pump, allowing a snug fit into a standard six-well cell culture plate (Figure 1F), and comprises an inlet and an outlet that enable media exchange without displacing the cortical organoid, ensuring stable experimental conditions.

To assess the suitability of the ion pump for modulating signaling in neuronal networks, we generated cortical organoids using mouse embryonic stem cells (ESCs) (Figure 2A).[38–40] We confirmed the presence of neuronal progenitors and neurons through immunohistochemical staining for Sox2 and Map2, respectively (Figure 2B). We confirmed the cortical identity of the organoids by immunohistochemistry for callosal (Satb2) and corticofugal excitatory projection neurons (Figure 2C). As previously reported, cortical organoids also have a subset of GABAergic interneurons, many of which are somatostatin (Sst) positive.[39–41] We confirmed the presence of these interneurons within our organoids (Figure 2D). For all experiments, we used 60- to 80-day-old cortical organoids to ensure maturity. This approach allowed us to study the effects of ionic pumps in 3D organoid systems that mimic functional neuronal networks in mice.

K^+ delivery using bioelectronic ionic pumps leads to rapid excitation of neuronal cells in cortical organoids

We set up the well plate with the 3D holder over a fluorescence microscope to demonstrate and monitor K^+ delivery from the ion pump to the cortical organoids in real time. We used alternating V_{K+} pulses of +1 and −1 V for 1 min over five cycles with the intent of adding and removing K^+ ions to the target solution. To monitor K^+ delivery, we measured the current (I_{k+}) between the WE and the RE (Figure 3A). A positive I_{k+} indicated delivery of K^+ from the reservoir into the target solution, and a negative I_{k+} indicated a current of K^+ moving from the target solution to the reservoir (Figure 3A). To quantify the delivery of K^+ ions, we measured the fluorescence intensity of a K^+ indicator, ION Potassium Green-2, as we pulsed V_{K+}.[24] By measuring this intensity and calibrating the fluorescence signal with solutions of known concentration (Figure S3A), we were able to plot the change in overall [K^+] in the target solution as a function of time, and we observed that V_{K+} = 1 V for 60 s changes [K^+] in the well by 3 mM (Figure 3B). One advantage of using the ion pump is that K^+ is delivered directly without the counterion, and even lower concentrations in the single mM range have been previously used to induce epileptic activity in hippocampal brain slices. In the future, improvements on ion pump geometry will afford

CellPress
OPEN ACCESS

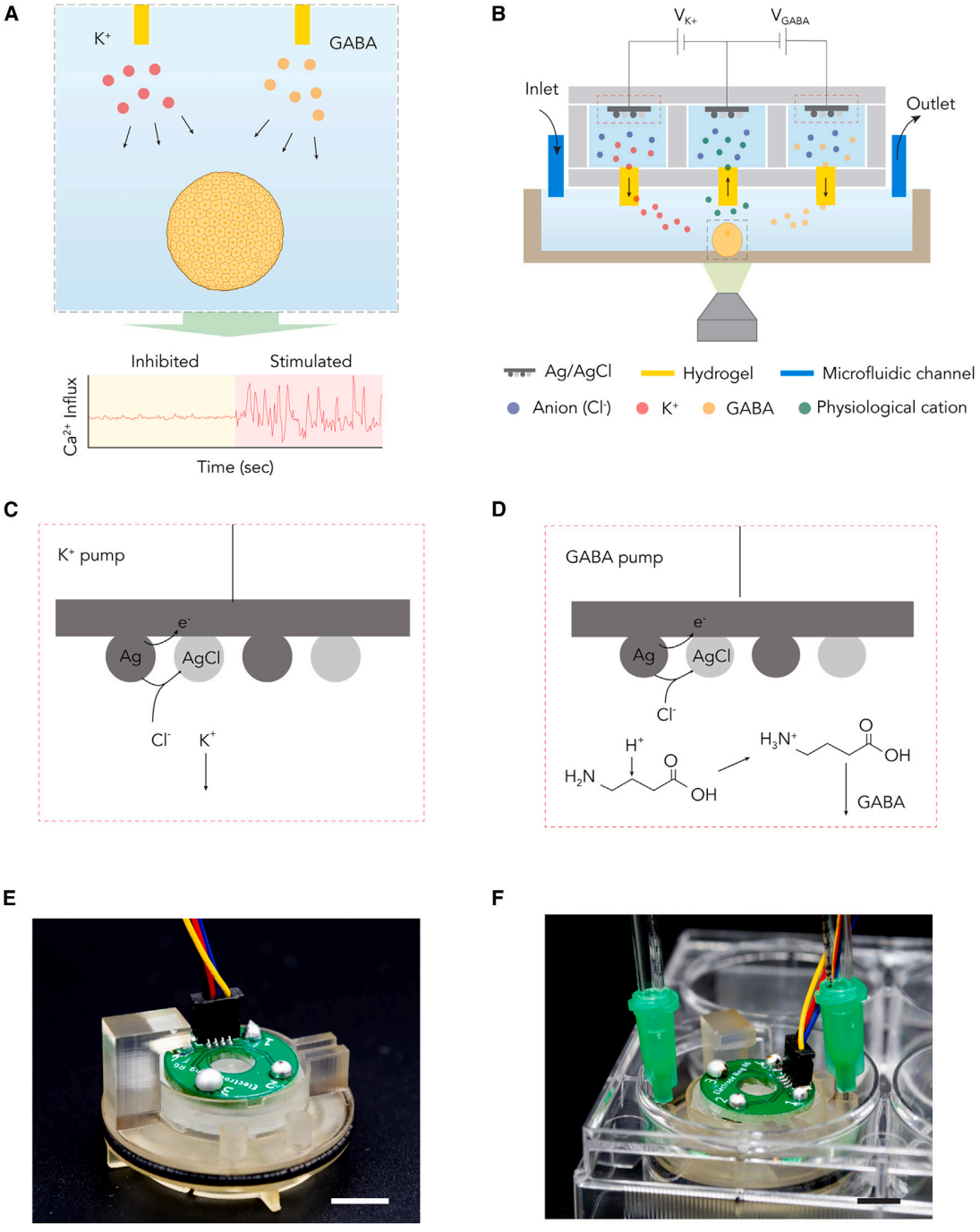

Figure 1. Experimental design

(A) Schematic representation of the bioelectronic ion pump for targeted delivery of K^+ and GABA. This is combined with a fluorescence microscope that enables real-time monitoring of the activity of the organoids via calcium imaging.

(B) A detailed schematic representation of the ion pump mechanism, illustrating the direction of ion movement during operation.

(C and D) Electrochemical reaction at the working electrode with (C) K^+ and (D) GABA molecules.

(E) Representative photo of the ion pump.

(F) Experimental setup with microfluidic channels. Scale bar: 1 cm.

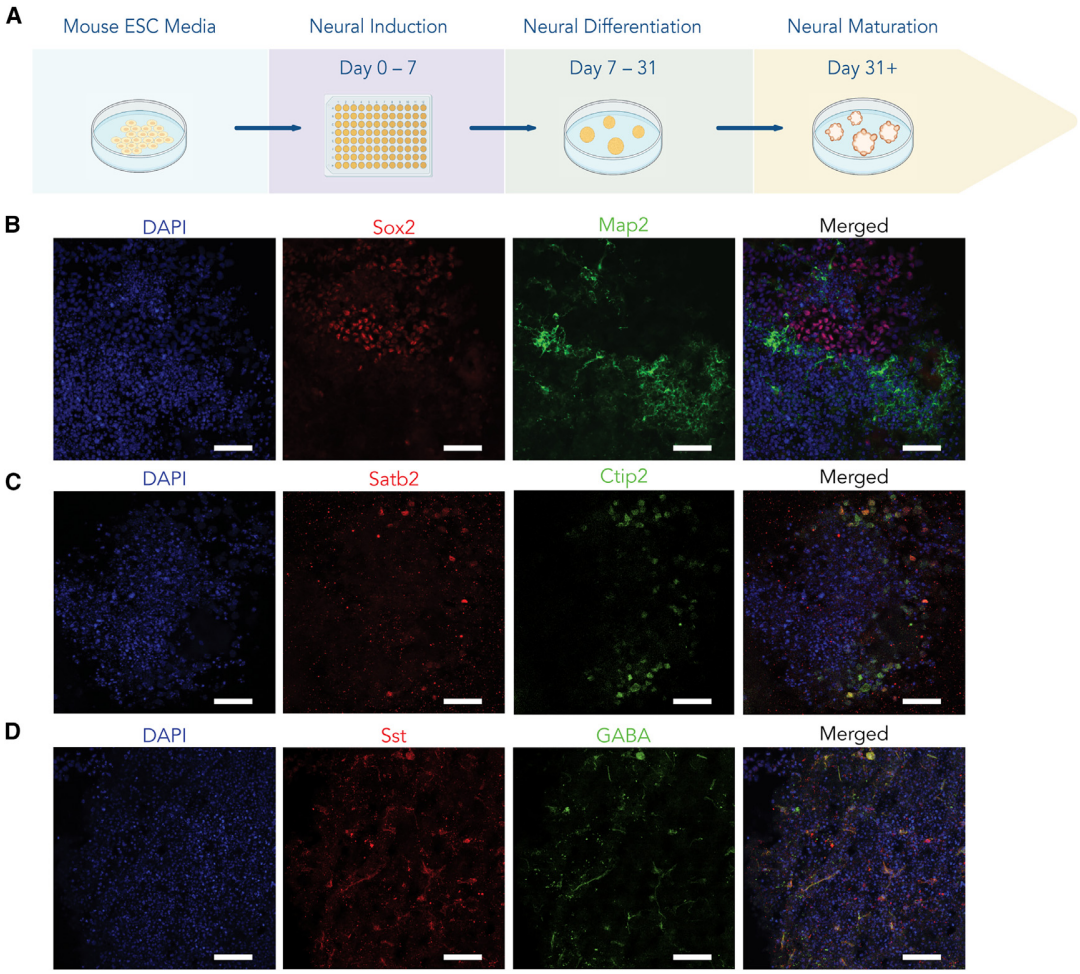

Figure 2. Generation of cortical organoids

(A) Schematic representing the protocol for cortical organoid generation and culture.

(B) Immunostaining of a cortical organoid showing the presence of neurons (Map2; green) and neuronal progenitors (Sox2; red).

(C) Immunostaining of a cortical organoid showing the presence of callosal (Satb2; red) and corticofugal (Ctip2; green) excitatory projection neurons.

(D) Immunostaining of a cortical organoid showing the presence of GABAergic neurons (GABA; green) and somatostatin (Sst; red). Nuclear counterstain is performed with DAPI. Scale bar: 50 μm.

delivering higher K^+ concentrations for acute stimulation experiments.

With this information in hand, we then evaluated the effect of the bioelectronic ion pump on neuronal activity of cortical organoids incubated with the non-ratiometric dye Fluo8AM, which enables the monitoring of intracellular Ca^{2+} ions.[42,43] We first recorded the spontaneous activity of the neurons within the organoid and selected a region of interest (ROI), highlighted in the figure by a white dotted line (Video S1; Figure 3C, left).

We then recorded the organoid activity as dF/F_0 as a function of time in the ROI in three sequential phases: the spontaneous activity phase (1 min), the ion pump on phase (1 min), and ion pump off followed by a wash off (1 min) (Figure 3C, left). During the first phase, all three organoids show a baseline spontaneous activity that is different from the others, as expected (Figure 3C, left). While we introduce K^+ in the well with V_{K+} = 1V (labeled as "K^+ on"), the activity for all three organoids visibly increases. An increase in [K^+] leads to an excitatory effect on the cortical organoid.[35,44] This excitatory effect is more evident when the data from Figure 3C are plotted in the frequency domain (Figure 3D) following the method by Sun et al.[45] At the end of the on phase, we set V_{K+} = 0 V and introduced new media from the inlet at 3 mL/min rate with the intent of flushing out any excessive K^+ from the solution surrounding the organoids. As expected in the "K^+ off," all three organoids eventually returned to a similar level of spontaneous activity as before (Figures 3C and 3D). Differences in how quickly and how closely the organoids returned to spontaneous activity can be attributed to different locations of the ROI with respect to the ion pump outlet, which would affect how the ions diffuse both during the delivery and the wash cycle, as well as variability in the organoids. Nonetheless, our

CellPress
OPEN ACCESS

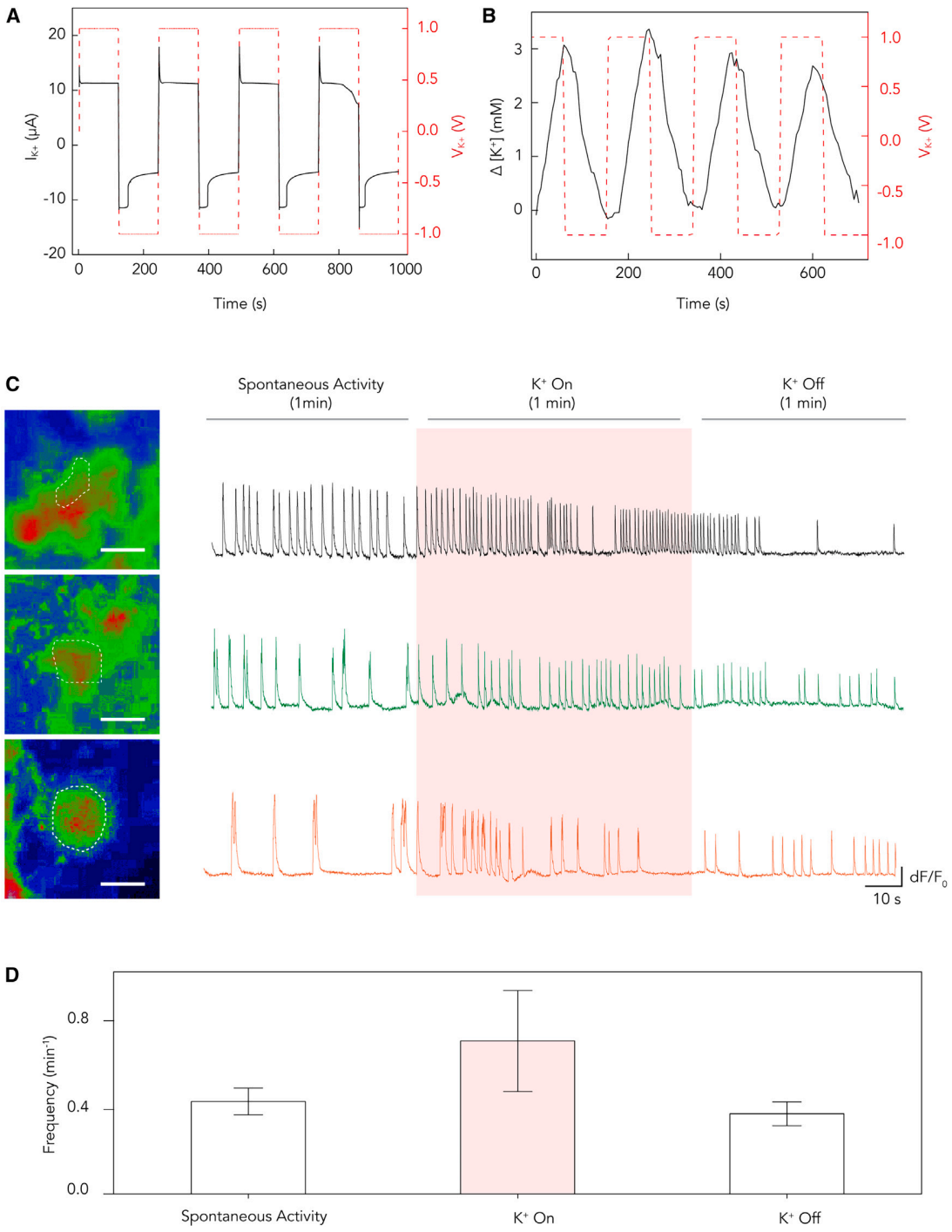

Figure 3. Bioelectronic delivery of K^+ ions to cortical organoids

(A) Electrical characterization of the bioelectronic ion pump, depicting the current response (I_{K+}) of the bioelectronic K^+ ion pump according to V_{K+}.

(B) Fluorescence response of bioelectronic K^+ ion pump in accordance with V_{K+}.

(C) Calcium imaging of organoids: (left) representative images of dF/F_0 (F = fluorescence intensity) representing calcium concentration and neuronal activity (scale bar: 10 μm). Dotted line highlights the ROI in which the traces on the right were recorded. (Right) A plot of fluorescence intensity versus time, illustrating the dynamic changes in neuronal activity during the K^+ delivery process.

(D) Analysis of the traces in (A) in the frequency domain by averaging the frequency for each organoid in the time period of 60 s. Scale bar represents standard deviation, n = 3 organoids from 3 different batches. Experiments were performed separately.

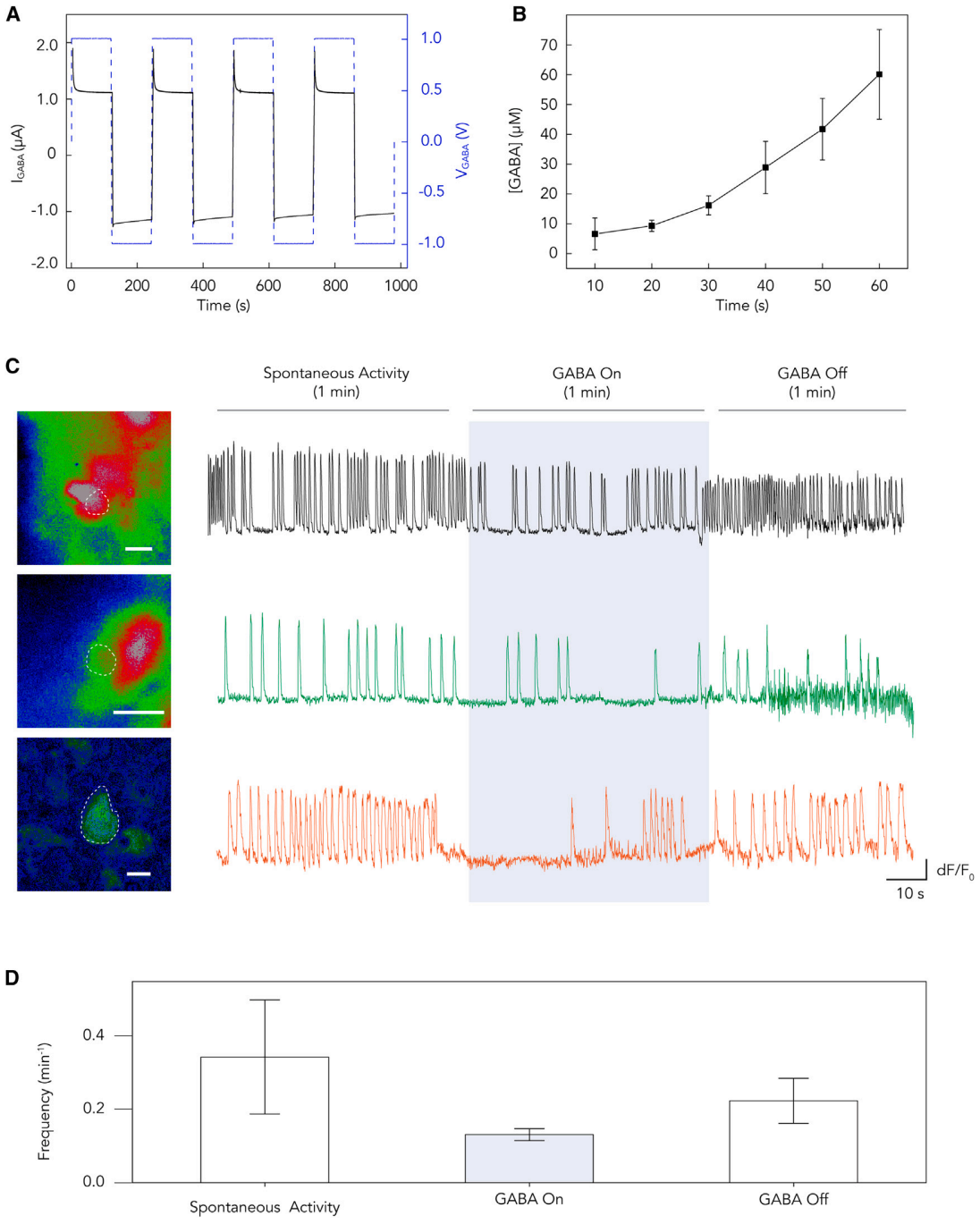

Figure 4. Bioelectronic delivery of GABA to cortical organoids

(A) Electrical characterization of the bioelectronic GABA ion pump, depicting the current response (I_{GABA}) of the bioelectronic GABA ion pump according to V_{GABA}.

(B) Liquid chromatography (LC) analysis of GABA concentration, demonstrating a detectable increase in concentration over a 1 min delivery period in response to V_{GABA}.

(C) Calcium imaging of organoids: (left) representative images of dF/F_0 representing calcium concentration and neuronal activity (scale bar: 10 μm). Dotted line highlights the ROI in which the traces on the right were recorded. (Right) A plot of fluorescence intensity versus time, illustrating the dynamic changes in neuronal activity during the GABA delivery process.

(D) Analysis of the traces in a in the frequency domain by averaging the frequency for each organoid in the time period of 60 s. Scale bar represents standard deviation, n = 3 organoids from 3 different batches. Experiments were performed separately.

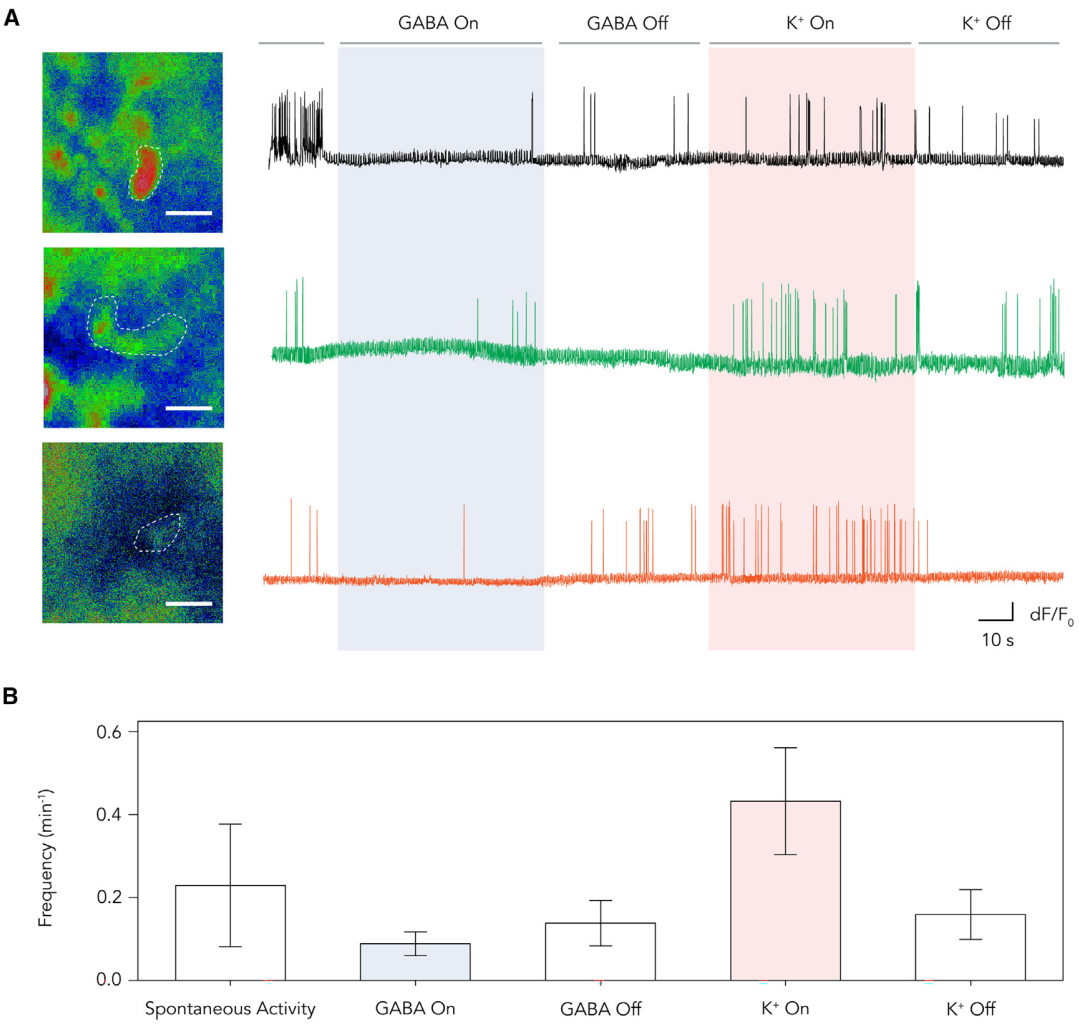

Figure 5. Sequential modulation of neural activity in cortical organoids using GABA and K^+ ions

(A) Calcium imaging of organoids: (left) representative images of dF/F_0 representing calcium concentration and neuronal activity (scale bar: 10 μm). Dotted line highlights the ROI in which the traces on the right were recorded. (Right) A plot of fluorescence intensity versus time, illustrating the dynamic changes in neuronal activity during the K^+ and GABA delivery process.

(B) Analysis of the traces in (A) in the frequency domain by averaging the frequency for each organoid in the time period of 60 s. Scale bar represents standard deviation, n = 3 organoids from 3 different batches. Experiments were performed separately.

measurements indicate that organoids increase in activity with K^+ delivery in a reversible fashion.

Bioelectronic pumps can effectively inhibit neuronal activity in brain organoids by delivering GABA

For the second set of experiments, we delivered the neurotransmitter GABA to the organoids with the ion pump (Figure 4). Pulsing V_{GABA} between +1 and −1 V results in I_{GABA} oscillating between 2 and −1 mA (Figure 4A). V_{GABA} = 1 V pushes GABA from the reservoir to the target solution, while V_{GABA} = −1 V drives positive charged ions from the target solution into the well. Since there is no direct way to measure the concentration of GABA in solution using a fluorescent dye, we measured how much GABA we delivered to the solution in the well with V_{GABA} = 1 V for different delivery durations (Figure 4B). Liquid chromatography indicated that delivering GABA for 60 s using the ion pump resulted in a GABA concentration of 60 μM in the 3 mL well (Figure S4B).

With these data in hand, we repeated the same procedure as K^+ with GABA (Figure 4C; Video S2). We were able to identify three ROIs with clearly visible spontaneous activity, which was reduced upon delivery of GABA for 1 min with V_{GABA} = 1V in the "GABA on" phase (Figures 4C and 4D) as expected due to GABA's inhibitory activity.[34] According to our liquid chromatography (LC) measurements, we expect the GABA concentration in the well to reach 60 mM after 60 s delivery. The observation of reduced activity is consistent with prior observations that GABA concentrations as low as 25 mM were successful at

reducing induced epileptic activity in hippocampal brain slices.[34] To ensure that the observed change in neuronal activity was indeed caused by the addition of K^+ and GABA to the solution containing organoids rather than the electrical stimulation from turning on the ion pump, we performed a control experiment in which the reservoir of the ion pump was filled with deionized (DI) water only (Video S3; Figure S4). As expected, this type of stimulation did not cause any change in organoid activity, confirming the effect of delivered K^+ and GABA.

Sequential GABA and K^+ delivery can rapidly modulate organoid activity

We investigated the effects of sequential delivery of GABA and K^+ (Figure 5). For this proof of concept, we designed five consecutive phases, each lasting 1 min: a spontaneous activity phase, a K^+ ion pump on phase, K^+ ion pump off with wash off, a GABA ion pump on phase, and GABA ion pump off with another rinse (Figure 5A). As expected, delivery of GABA with the ion pump for 1 min resulted in a reduction of activity that returned to the normal state after the solution was replaced for 1 min while the ion pump was turned off (Figures 5A and 5B). Subsequent addition of K^+ resulted in increased activity as previously demonstrated (Figures 5A and 5B). This proof-of-concept sequential delivery further demonstrated the ability of our system to control the activity of organoids with delivery of different biochemicals. While this is only a short-term study, the ion pumps can deliver K^+ and GABA for extended periods of time (Figures S5A and S5B), and the overall system is compatible with an incubator, allowing for future studies of longer duration.

DISCUSSION

The ability to rapidly manipulate organoid activity can have direct applications in both fundamental and translational biology.[24,26,46] In this work, we have demonstrated the application of a bioelectronic ion pump to increase and inhibit neuronal activity with the targeted delivery of K^+ and GABA to cortical organoids. Using calcium transients as the readout for baseline neuronal activity, we delivered K^+ ions to increase activity and GABA to inhibit neuronal activity. We observed that the organoids returned to their initial state upon washing with fresh media, indicating the potential for reversible experiments. This work marks a significant advancement over current approaches, which often introduce pharmacological agents through bath applications requiring lengthy incubation periods for agent diffusion.[5] Considering the rapid return to the baseline state, this bioelectronic approach could facilitate chronic electrophysiology experiments, currently limited to recording the spontaneous activity of the organoids.[4,47] In the future, the integration of bioelectronic ion pumps with a broader range of ions and charged molecules, including Na^+, H^+, serotonin, dopamine, and zolmitriptan, will provide new opportunities to study circuit maturation and plasticity. This promises to further our understanding and provide tools for more precise manipulations in both fundamental and applied neurological research.

Limitation of the study

One area that needs improvement in the proposed method is the management of temperature and gas-exchange conditions during calcium imaging when having the ion pump and the microfluidic system over the well plate. After 3 min, it is noticeable that the signal-to-noise ratio decreases because of intensity decay of the fluorescence. To address this issue and prevent activity decline due to inadequate gas exchange and temperature, we are actively devising strategies to conduct calcium imaging in conditions similar to an incubator while incorporating the microfluidics and ion pump system described. Future platforms will benefit from more precise spatial control of the ion concentration[30,31] matched with multielectrode arrays to better control stimuli and activity recording.

STAR★METHODS

Detailed methods are provided in the online version of this paper and include the following:

- KEY RESOURCES TABLE
- RESOURCE AVAILABILITY
  - Lead contact
  - Materials availability
  - Data and code availability
- EXPERIMENTAL MODEL AND STUDY PARTICIPANT DETAILS
  - ESC culture
- METHOD DETAILS
  - Cortical organoids generation
  - Ion pump fabrication
  - Device characterization
  - Calcium imaging
  - Ion delivery using the bioelectronic ion pump
- QUANTIFICATION AND STATISTICAL ANALYSIS

SUPPLEMENTAL INFORMATION

Supplemental information can be found online at https://doi.org/10.1016/j.crmeth.2023.100686.

ACKNOWLEDGMENTS

This work was supported by Schmidt Futures (SF857) to S.R.S. and M.T., the National Human Genome Research Institute (1RM1HG011543) to S.R.S. and M.T., the National Science Foundation (NSF2134955) to S.R.S. and M.T., and the National Institute of Mental Health (1U24MH132628) to M.A.M.-R. K.V. was supported by the ARCS Foundation and grant T32HG012344 from the National Human Genome Research Institute (NHGRI), part of the National Institutes of Health (NIH), USA. H.E.S. is a National Science Foundation Graduate Research Fellowship grantee. M.R. acknowledges support from the Defense Advanced Research Projects Agency (DARPA) through cooperative agreement no. D20AC00003 awarded by the US Department of the Interior (DOI) and the Interior Business Center and the Army Research Office (ARO) through contract no. W911NF2210058 issued by US Army ACC-APG-RTP W911NF. The content of the article does not necessarily reflect the position or the policy of the government, and no official endorsement should be inferred. Microfabrication was performed using equipment sponsored by the W.M. Keck Center for Nanoscale Optofluidics, the California Institute for Quantitative Biosciences (QB3), and the Army Research Office, award no. W911NF-17-1-0460.

AUTHOR CONTRIBUTIONS

Y.P. carried out the majority of the experiments, data analysis, and manuscript preparation. S.H. performed calcium imaging and contributed to the biological aspects of the study. C.O.H. was responsible for the fabrication of the bioelectronic ion pump device. H.E.S. conducted organoid imaging and calcium imaging. K.V., H.L., H.D., N.H., E.M.M., and F.N.S. provided valuable feedback and suggestions on the experimental design and manuscript. R.U. and S.R.S. contributed by securing funding for the project. H.J.K. performed control experiments and imaging of the device. M.T., M.A.M.-R., and M.R. provided supervision, guidance, and conceptual ideas for the project; contributed to manuscript writing, editing, and revisions; and procured funding for the research.

DECLARATION OF INTERESTS

The authors declare no competing interests.

Received: July 11, 2023
Revised: November 1, 2023
Accepted: December 14, 2023
Published: January 12, 2024

REFERENCES

1. Nowakowski, T.J., and Salama, S.R. (2022). Cerebral Organoids as an Experimental Platform for Human Neurogenomics. Cells *11*, 2803.
2. Mostajo-Radji, M.A., Schmitz, M.T., Montoya, S.T., and Pollen, A.A. (2020). Reverse engineering human brain evolution using organoid models. Brain Res. *1729*, 146582.
3. Quadrato, G., Nguyen, T., Macosko, E.Z., Sherwood, J.L., Min Yang, S., Berger, D.R., Maria, N., Scholvin, J., Goldman, M., Kinney, J.P., et al. (2017). Cell diversity and network dynamics in photosensitive human brain organoids. Nature *545*, 48–53.
4. Sharf, T., Van Der Molen, T., Glasauer, S.M.K., Guzman, E., Buccino, A.P., Luna, G., Cheng, Z., Audouard, M., Ranasinghe, K.G., Kudo, K., et al. (2022). Functional neuronal circuitry and oscillatory dynamics in human brain organoids. Nat. Commun. *13*, 4403.
5. Trujillo, C.A., Gao, R., Negraes, P.D., Gu, J., Buchanan, J., Preissl, S., Wang, A., Wu, W., Haddad, G.G., Chaim, I.A., et al. (2019). Complex Oscillatory Waves Emerging from Cortical Organoids Model Early Human Brain Network Development. Cell Stem Cell *25*, 558–569.e7.
6. Zafeiriou, M.-P., Bao, G., Hudson, J., Halder, R., Blenkle, A., Schreiber, M.-K., Fischer, A., Schild, D., and Zimmermann, W.-H. (2020). Developmental GABA polarity switch and neuronal plasticity in Bioengineered Neuronal Organoids. Nat. Commun. *11*, 3791.
7. Popova, G., Soliman, S.S., Kim, C.N., Keefe, M.G., Hennick, K.M., Jain, S., Li, T., Tejera, D., Shin, D., Chhun, B.B., et al. (2021). Human microglia states are conserved across experimental models and regulate neural stem cell responses in chimeric organoids. Cell Stem Cell *28*, 2153–2166.e6.
8. Birey, F., Andersen, J., Makinson, C.D., Islam, S., Wei, W., Huber, N., Fan, H.C., Metzler, K.R.C., Panagiotakos, G., Thom, N., et al. (2017). Assembly of functionally integrated human forebrain spheroids. Nature *545*, 54–59.
9. Xu, Y.-J., Liu, P.-P., Yan, Z.-Z., Mi, T.-W., Wang, Y.-Y., Li, Q., Teng, Z.-Q., and Liu, C.-M. (2022). KW-2449 and VPA exert therapeutic effects on human neurons and cerebral organoids derived from MECP2-null hESCs. Stem Cell Res. Ther. *13*, 534.
10. Hergenreder, E., Zorina, Y., Zhao, Z., Munguba, H., Calder, E.L., Baggiolini, A., Minotti, A.P., Walsh, R.M., Liston, C., Levitz, J., et al. (2022). Combined Small Molecule Treatment Accelerates Timing of Maturation in Human Pluripotent Stem Cell-Derived Neurons (Cold Spring Harbor Laboratory).
11. Jabaudon, D. (2017). Fate and freedom in developing neocortical circuits. Nat. Commun. *8*, 16042.
12. Martini, F.J., Guillamón-Vivancos, T., Moreno-Juan, V., Valdeolmillos, M., and López-Bendito, G. (2021). Spontaneous activity in developing thalamic and cortical sensory networks. Neuron *109*, 2519–2534.
13. Molnár, Z., Luhmann, H.J., and Kanold, P.O. (2020). Transient cortical circuits match spontaneous and sensory-driven activity during development. Science *370*, eabb2153.
14. Bando, Y., Hirano, T., and Tagawa, Y. (2014). Dysfunction of KCNK Potassium Channels Impairs Neuronal Migration in the Developing Mouse Cerebral Cortex. Cereb. Cortex *24*, 1017–1029.
15. Barel, O., Shalev, S.A., Ofir, R., Cohen, A., Zlotogora, J., Shorer, Z., Mazor, G., Finer, G., Khateeb, S., Zilberberg, N., and Birk, O.S. (2008). Maternally Inherited Birk Barel Mental Retardation Dysmorphism Syndrome Caused by a Mutation in the Genomically Imprinted Potassium Channel KCNK9. Am. J. Hum. Genet. *83*, 193–199.
16. Smith, R.S., Kenny, C.J., Ganesh, V., Jang, A., Borges-Monroy, R., Partlow, J.N., Hill, R.S., Shin, T., Chen, A.Y., Doan, R.N., et al. (2018). Sodium Channel SCN3A (NaV1.3) Regulation of Human Cerebral Cortical Folding and Oral Motor Development. Neuron *99*, 905–913.e7.
17. Avila, A., Vidal, P.M., Dear, T.N., Harvey, R.J., Rigo, J.-M., and Nguyen, L. (2013). Glycine receptor α2 subunit activation promotes cortical interneuron migration. Cell Rep. *4*, 738–750.
18. LoTurco, J.J., Owens, D.F., Heath, M.J., Davis, M.B., and Kriegstein, A.R. (1995). GABA and glutamate depolarize cortical progenitor cells and inhibit DNA synthesis. Neuron *15*, 1287–1298.
19. Murthy, S., Niquille, M., Hurni, N., Limoni, G., Frazer, S., Chameau, P., Van Hooft, J.A., Vitalis, T., and Dayer, A. (2014). Serotonin receptor 3A controls interneuron migration into the neocortex. Nat. Commun. *5*, 5524.
20. Ojeda, J., and Ávila, A. (2019). Early Actions of Neurotransmitters During Cortex Development and Maturation of Reprogrammed Neurons. Front. Synaptic Neurosci. *11*, 33.
21. Wang, D.D., and Kriegstein, A.R. (2009). Defining the role of GABA in cortical development. J. Physiol. *587*, 1873–1879.
22. Lancaster, M.A., Renner, M., Martin, C.-A., Wenzel, D., Bicknell, L.S., Hurles, M.E., Homfray, T., Penninger, J.M., Jackson, A.P., and Knoblich, J.A. (2013). Cerebral organoids model human brain development and microcephaly. Nature *501*, 373–379.
23. Del Dosso, A., Urenda, J.-P., Nguyen, T., and Quadrato, G. (2020). Upgrading the Physiological Relevance of Human Brain Organoids. Neuron *107*, 1014–1028.
24. Dechiraju, H., Selberg, J., Jia, M., Pansodtee, P., Li, H., Hsieh, H.-C., Hernandez, C., Asefifeyzabadi, N., Nguyen, T., Baniya, P., et al. (2022). On-chip on-demand delivery of K^+ for *in vitro* bioelectronics. AIP Adv. *12*, 125205.
25. Isaksson, J., Kjäll, P., Nilsson, D., Robinson, N.D., Berggren, M., and Richter-Dahlfors, A. (2007). Electronic control of Ca2+ signalling in neuronal cells using an organic electronic ion pump. Nat. Mater. *6*, 673–679.
26. Dechiraju, H., Jia, M., Luo, L., and Rolandi, M. (2022). Ion-Conducting Hydrogels and Their Applications in Bioelectronics. Advanced Sustainable Systems *6*, 2100173.
27. Jia, M., Dechiruji, H., Selberg, J., Pansodtee, P., Mathews, J., Wu, C., Levin, M., Teodorescu, M., and Rolandi, M. (2020). Bioelectronic control of chloride ions and concentration with Ag/AgCl contacts. Apl. Mater. *8*.
28. Selberg, J., Jafari, M., Bradley, C., Gomez, M., and Rolandi, M. (2020). Expanding biological control to bioelectronics with machine learning. Apl. Mater. *8*, 120904.
29. Selberg, J., Jafari, M., Mathews, J., Jia, M., Pansodtee, P., Dechiraju, H., Wu, C., Cordero, S., Flora, A., Yonas, N., et al. (2020). Machine Learning-Driven Bioelectronics for Closed-Loop Control of Cells. Advanced Intelligent Systems *2*, 2000140.
30. Jia, M., Jafari, M., Pansodtee, P., Teodorescu, M., Gomez, M., and Rolandi, M. (2022). A multi-ion electrophoretic pump for simultaneous on-chip delivery of H+, Na+, and Cl−. Apl. Mater. *10*, 041112.

31. Park, Y., Luo, L., and Rolandi, M. (2023). Integrating Ion Channels with Bioelectronics for Biotic–Abiotic Systems. Advanced Intelligent Systems *5*.

32. Seitanidou, M., Blomgran, R., Pushpamithran, G., Berggren, M., and Simon, D.T. (2019). Modulating Inflammation in Monocytes Using Capillary Fiber Organic Electronic Ion Pumps. Adv. Healthc. Mater. *8*, 1900813.

33. Hosseini Jafari, B., Zlobina, K., Marquez, G., Jafari, M., Selberg, J., Jia, M., Rolandi, M., and Gomez, M. (2021). A feedback control architecture for bioelectronic devices with applications to wound healing. J. R. Soc. Interface *18*, 20210497.

34. Williamson, A., Rivnay, J., Kergoat, L., Jonsson, A., Inal, S., Uguz, I., Ferro, M., Ivanov, A., Sjöström, T.A., Simon, D.T., et al. (2015). Controlling Epileptiform Activity with Organic Electronic Ion Pumps. Adv. Mater. *27*, 3138–3144.

35. Filosa, J.A., Bonev, A.D., Straub, S.V., Meredith, A.L., Wilkerson, M.K., Aldrich, R.W., and Nelson, M.T. (2006). Local potassium signaling couples neuronal activity to vasodilation in the brain. Nat. Neurosci. *9*, 1397–1403.

36. Somjen, G.G. (1979). Extracellular Potassium in the Mammalian Central Nervous System. Annu. Rev. Physiol. *41*, 159–177.

37. Nguyen, T., Asefifeyzabadi, N., Li, H., Luo, L., and Rolandi, M. (2023). The Importance of Electrode Material in Bioelectronic Electrophoretic Ion Pumps. Adv. Mater. Technol. *8*, 2201996.

38. Seitanidou, M., Franco-Gonzalez, J.F., Sjöström, T.A., Zozoulenko, I., Berggren, M., and Simon, D.T. (2017). pH Dependence of γ-Aminobutyric Acid Iontronic Transport. J. Phys. Chem. B *121*, 7284–7289.

39. Kadoshima, T., Sakaguchi, H., Nakano, T., Soen, M., Ando, S., Eiraku, M., and Sasai, Y. (2013). Self-organization of axial polarity, inside-out layer pattern, and species-specific progenitor dynamics in human ES cell–derived neocortex. Proc. Natl. Acad. Sci. USA *110*, 20284–20289.

40. Pollen, A.A., Bhaduri, A., Andrews, M.G., Nowakowski, T.J., Meyerson, O.S., Mostajo-Radji, M.A., Di Lullo, E., Alvarado, B., Bedolli, M., Dougherty, M.L., et al. (2019). Establishing Cerebral Organoids as Models of Human-Specific Brain Evolution. Cell *176*, 743–756.e17.

41. Velasco, S., Kedaigle, A.J., Simmons, S.K., Nash, A., Rocha, M., Quadrato, G., Paulsen, B., Nguyen, L., Adiconis, X., Regev, A., et al. (2019). Individual brain organoids reproducibly form cell diversity of the human cerebral cortex. Nature *570*, 523–527.

42. Grienberger, C., and Konnerth, A. (2012). Imaging Calcium in Neurons. Neuron *73*, 862–885.

43. Lock, J.T., Parker, I., and Smith, I.F. (2015). A comparison of fluorescent Ca2+ indicators for imaging local Ca2+ signals in cultured cells. Cell Calcium *58*, 638–648.

44. Yao, H., Wu, W., Cerf, I., Zhao, H.W., Wang, J., Negraes, P.D., Muotri, A.R., and Haddad, G.G. (2020). Methadone interrupts neural growth and function in human cortical organoids. Stem Cell Res. *49*, 102065.

45. Sun, Z., and Südhof, T.C. A simple Ca(2+)-imaging approach to neural network analyses in cultured neurons

46. Zhang, Y.S., Aleman, J., Shin, S.R., Kilic, T., Kim, D., Mousavi Shaegh, S.A., Massa, S., Riahi, R., Chae, S., Hu, N., et al. (2017). Multisensor-integrated organs-on-chips platform for automated and continual in situ monitoring of organoid behaviors. Proc. Natl. Acad. Sci. USA *114*, E2293–E2302.

47. Le Floch, P., Li, Q., Lin, Z., Zhao, S., Liu, R., Tasnim, K., Jiang, H., and Liu, J. (2022). Stretchable Mesh Nanoelectronics for 3D Single-Cell Chronic Electrophysiology from Developing Brain Organoids. Adv. Mater. *34*, 2106829.

48. Pansodtee, P., Selberg, J., Jia, M., Jafari, M., Dechiraju, H., Thomsen, T., Gomez, M., Rolandi, M., and Teodorescu, M. (2021). The multi-channel potentiostat: Development and evaluation of a scalable mini-potentiostat array for investigating electrochemical reaction mechanisms. PLoS One *16*, e0257167.

STAR★METHODS

KEY RESOURCES TABLE

REAGENT or RESOURCE	SOURCE	IDENTIFIER
Antibodies		
Rabbit anti-GABA polyclonal antibody	Thermo Fisher	Cat# PA5-32241; RRID: AB_2549714
Mouse anti-somatostatin monoclonal antibody	Santa Cruz Biotechnology	Cat# sc55565; RRID: AB_831726
Rat anti-ctip2 monoclonal antibody	Abcam	Cat# ab18465; RRID: AB_2064130
Mouse anti-satb2 monoclonal antibody	Abcam	Cat# ab51502; RRID: AB_882455
Rabbit anti-map2 polyclonal antibody	Proteintech	Cat# 17490-1-AP; RRID: AB_2137880
Mouse anti-sox2 monoclonal antibody	Santa Cruz Biotechnology	Cat# sc365823; RRID: AB_10842165
Chemicals, peptides, and recombinant proteins		
DAPI (4′,6-Diamidino-2-Phenylindole, Dihydrochloride)	Life Technologies Corporation	D1306
Vitronectin	Thermo Fischer	A14700
Glasgow Minimum Essential Medium	Thermo Fisher	11710035
Embryonic Stem Cell-Qualified Fetal Bovine Serum	Thermo Fisher	10439001
MEM Non-Essential Amino Acids	Thermo Fisher	11140050
Sodium Pyruvate	Millipore Sigma	S8636
Glutamax supplement	Thermo Fisher	35050061
2-Mercaptoethanol	Millipore Sigma	M3148
Primocin	Invitrogen	ant-pm-05
Recombinant Mouse Leukemia Inhibitory Factor	Millipore Sigma	ESG1107
ReLeSR passaging reagent	Stem Cell Technologies	05872
mFreSR cryopreservation medium	Stem Cell Technologies	05855
Rho Kinase Inhibitor (Y-27632)	Tocris	1254
WNT inhibitor (IWR1-ε)	Cayman Chemical	13659
TGF-Beta inhibitor (SB431542)	Tocris	1614
Dulbecco's Modified Eagle Medium: Nutrient Mixture F-12 with GlutaMAX supplement	Thermo Fisher	10565018
N-2 Supplement	Thermo Fisher	17502048
Chemically Defined Lipid Concentrate	Thermo Fisher	11905031
Heparin sodium salt	Millipore Sigma	M3148
Matrigel Growth Factor Reduced (GFR) Basement Membrane Matrix	Corning	354230
BrainPhys Neuronal Medium	Stem Cell Technologies	05790
BrainPhys Imaging Optimized Medium	Stem Cell Technologies	5796
B-27 Supplement	Thermo Fisher	17504044
Fluo-8 a.m.	Abcam	ab142773
IPG-2 a.m.	Cayman Chemical	35540
Photoinitiator (I2959)	Millipore Sigma	410896
2-acrylamido-2-methyl-1-propanesulfonic acid	Millipore Sigma	282731
PDMS	Dow corning	Sylgard 184
KCl (Potassium Chloride)	Millipore Sigma	P9333
GABA(γ-Aminobutyric Acid)	Millipore Sigma	A2129
Experimental models: Cell lines		
ES-E14TG2a Mouse Embryonic Stem Cell	ATCC	ATCC CRL-1821
Software and algorithms		
ImageJ software, 1.53p	ImageJ	https://ImageJ.nih.gov/ij
VirtualDub software	VirtualDub	https://www.virtualdub.org

(*Continued on next page*)

Continued

REAGENT or RESOURCE	SOURCE	IDENTIFIER
Other		
EVOS M7000 Imaging System	Invitrogen	AMF7000
GFP light cube	Invitrogen	AMEP4651
VWR minipump variable flow	Avantor	Model 3385

RESOURCE AVAILABILITY

Lead contact

Further information and requests for resources and reagents should be directed to and will be fulfilled by the lead contact, Marco Rolandi (mrolandi@ucsc.edu).

Materials availability

This study did not generate new unique reagents.

Data and code availability

- All data are available in the main text and supplementary information.
- This paper does not report original code.
- Any additional information required to reanalyze the data reported in this work paper is available from the lead contact upon request.

EXPERIMENTAL MODEL AND STUDY PARTICIPANT DETAILS

ESC culture

All experiments were performed in the ES-E14TG2a mouse Embryonic Stem Cell (ESC) line (ATCC CRL-1821). This line is derived from a male of the 129/Ola mouse strain. Mycoplasma testing confirmed lack of contamination. ESCs were maintained on Recombinant Human Protein Vitronectin (Thermo Fischer # A14700) coated plates using mESC maintenance media containing Glasgow Minimum Essential Medium (Thermo Fisher Scientific # 11710035), Embryonic Stem Cell-Qualified Fetal Bovine Serum (Thermo Fisher Scientific # 10439001), 0.1 mM MEM Non-Essential Amino Acids (Thermo Fisher Scientific # 11140050), 1 mM Sodium Pyruvate (Millipore Sigma #S8636), 2 mM Glutamax supplement (Thermo Fisher Scientific # 35050061), 0.1 mM 2-Mercaptoethanol (Millipore Sigma #M3148), and 0.05 mg/mL Primocin (Invitrogen # ant-pm-05). mESC maintenance media was supplemented with 1,000 units/mL of Recombinant Mouse Leukemia Inhibitory Factor (Millipore Sigma # ESG1107). Media was changed daily. Vitronectin coating was incubated for 15 min at a concentration of 0.5 μg/mL dissolved in 1X Phosphate-buffered saline (PBS) pH 7.4 (Thermo Fisher Scientific # 70011044). Dissociation and cell passages were done using ReLeSR passaging reagent (Stem Cell Technologies # 05872) according to manufacturer's instructions. Cell freezing was done in mFreSR cryopreservation medium (Stem Cell Technologies # 05855) according to manufacturer's instructions.

METHOD DETAILS

Cortical organoids generation

To generate cortical organoids, we clump-dissociated ESCs using ReLeSR and re-aggregated in lipidure-coated 96-well V-bottom plates at a density of 10,000 cells per aggregate, in 200 μL of mESC maintenance media supplemented with Rho Kinase Inhibitor (Y-27632, 10 μM, Tocris # 1254) (Day −1). After one day (Day 0), we replaced the medium with cortical differentiation medium containing Glasgow Minimum Essential Medium (Thermo Fisher Scientific # 11710035), 10% Knockout Serum Replacement (Thermo Fisher Scientific # 10828028), 0.1 mM MEM Non-Essential Amino Acids (Thermo Fisher Scientific # 11140050), 1 mM Sodium Pyruvate (Millipore Sigma #S8636), 2 mM Glutamax supplement (Thermo Fisher Scientific # 35050061) 0.1 mM 2-Mercaptoethanol (Millipore Sigma #M3148) and 0.05 mg/mL Primocin (Invitrogen # ant-pm-05).

Cortical differentiation medium was supplemented with Rho Kinase Inhibitor (Y-27632, 20 μM # 1254), WNT inhibitor (IWR1-ε, 3 μM, Cayman Chemical # 13659) and TGF-Beta inhibitor (SB431542, Tocris # 1614, 5 μM, days 0–7). Media was changed on days 3 and 6 and then every 2–3 days until day 7. On day 7 organoids were transferred to ultra-low adhesion plates (Millipore Sigma # CLS3471) and put on an orbital shaker in neuronal differentiation medium at 75 revolutions per minute. Neuronal differentiation medium contained Dulbecco's Modified Eagle Medium: Nutrient Mixture F-12 with GlutaMAX supplement (Thermo Fisher Scientific # 10565018), 1X N-2 Supplement (Thermo Fisher Scientific # 17502048), 1X Chemically Defined Lipid Concentrate (Thermo Fisher Scientific # 11905031) and 0.05 mg/mL Primocin (Invitrogen # ant-pm-05). Organoids were grown under 40% O_2 and 5% CO_2 conditions. Medium was changed every 2–3 days. On day 14 onward, we added 5 μg/mL Heparin sodium salt from porcine intestinal

mucosa (Millipore Sigma #H3149) and 0.5% v/v Matrigel Growth Factor Reduced (GFR) Basement Membrane Matrix, LDEV-free (Matrigel GFR, Corning # 354230) to the neuronal differentiation medium. On day 21 onward, we transferred the organoids to neuronal maturation media containing BrainPhys Neuronal Medium (Stem Cell Technologies # 05790), 1X N-2 Supplement, 1X Chemically Defined Lipid Concentrate (Thermo Fisher Scientific # 11905031), 1X B-27 Supplement (Thermo Fisher Scientific # 17504044), 0.05 mg/mL Primocin (Invitrogen # ant-pm-05). and 1% v/v Matrigel Growth Factor Reduced (GFR) Basement Membrane Matrix, LDEV-free.

Ion pump fabrication

We created PDMS molds by utilizing Preform software in conjunction with Form3 3D printers. These molds consist of two distinct layers: the lower layer defining the reservoirs and the upper layer serving as the lid to seal these reservoirs. After demolding the PDMS, we inserted Ag and AgCl wires into the reservoirs (250 mm diameter, 7 mm length) to create the electrodes. Subsequently, we joined the two PDMS layers, treating the contact interfaces with 50 W oxygen plasma for 10 s and securing them together using custom-made aluminum clamps. Following the bonding process, a 1.5 μm thick water-insulating layer of Parylene-C was deposited, using the Specialty Coating Systems Lab Coater, in the presence of an A174 adhesion promoter. This layer also serves the purpose of preventing the formation of bubbles in the reservoir. Four 3 mm long hydrogel-filled capillaries were then inserted through the PDMS, and the reservoirs were filled with a 1M KCl or 100mM GABA solution using a syringe. To secure the device within a custom-made 3D printed adapter, specifically designed for anchoring the device in 6-well cell culture plates, we applied a layer of uncured PDMS at the interface. This uncured PDMS was allowed to cure for 48 h at room temperature, ensuring a water-tight seal. The hydrogel recipe used in this study included a 1 M concentration of 2-acrylamido-2-methyl-1-propanesulfonic acid (AMPSA), 0.4 M concentration of polyethylene glycol diacrylate (AMPSA), and 0.05 M concentration of photoinitiator (I2959). Silica tubing measuring 100 mm with an inner diameter of 100 μm and an outer diameter of 375 μm underwent etching with NaOH and was then treated with silane A174 to prevent hydrogel expansion. The hydrogel was crosslinked through 5 min of exposure to 365 nm UV light at a power density of 8 mW cm-2. After UV curing, the capillary tubes were segmented into 7 mm sections and loaded by immersing them in either a 1M KCl solution or a 10mM GABA solution for at least 4 h before use. The ring-shaped PCB board featured four plated through holes as the insertion points for dowel pins. These pins, in turn, were connected to the control board through a JST-SH 4-pin connector, establishing a secure and reliable electrical connection between the electrodes and the control board. The control board is a 16-channel potentiostat integrated with a Raspberry Pi single-board computer, following the design outlined by Pansodtee et al.[48] Each channel generates an actuation voltage within the range of ±4 V and delivers an output current of ±20 μA. To monitor real-time current, the controller employs an instrumental amplifier, which initially measures the voltage across a high-precision (0.1%) 1 kΩ shunt resistor. Subsequently, the onboard ADS1115 analog-to-digital converters (ADCs) are utilized to gauge the output voltages of the amplifiers and ascertain the corresponding currents. For setting the actuation voltages, the system relies on the onboard MCP4728 digital-to-analog converters (DACs). Communication with these components is facilitated through the I2C communication bus of the Raspberry Pi, allowing for command transmission to the DACs and retrieval of data from the ADCs. Running on the Raspberry Pi is a Python program that awaits commands from a client, enabling adjustments to the actuation voltages and the measurement of currents.

Device characterization

To monitor the variation in K^+ ion and GABA concentration, we employed microscopy for real-time imaging and LC measurements. For K^+ ions, we utilized IPG-2 dye, an intracellular K^+ indicator optimized to a concentration of 3 μM in 0.1M Tris buffer. This dye, characterized by excitation and emission wavelengths of 525 nm and 545 nm, respectively, exhibits a linear relationship between fluorescence intensity and K^+ concentration, thereby enabling the detection of subtle shifts in K^+ levels. To quantify this delivery, we derived a calibration curve using the fluorescent responses of solutions with known K^+ ion concentrations ranging from 0 to 150 mM, illustrated in Figure S4A. Notably, between concentrations of 0–50 mM, there was a consistent increase in fluorescence intensity. During a 1-min actuation period, we measured the fluorescence intensity (Figure 3B). By cross-refencing this measurement with our calibration data, we determined that the ion pump effectively delivered enough K^+ to change the concentration in the reservoir by 3 mM. The data collected were analyzed using ImageJ 1.53p version. For GABA quantification, LC measurement was carried out using LC-MS (LTQ-Orbitrap, Thermo, USA)

Calcium imaging

The day before imaging, the organoids were switched to maturation media in which BrainPhys Neuronal Media was replaced with BrainPhys Imaging Optimized Medium (Stem Cell Technologies # 5796). Calcium imaging was done using 4 μM Fluo-8 a.m. (Abcam # ab142773). The organoids were incubated at 37°C with Fluo-8 a.m. for 30 min before imaging. Calcium imaging was performed using an inverted fluorescence microscope (EVOS M7000 Imaging System, Invitrogen, USA). All the videos and images acquisitions were executed using objectives with magnifications of either 10× and 20X (Olympus, Japan). To ensure optimal fluorescence detection, we employed a Green fluorescent light cube (GFP light cube; AMEP4651, Invitrogen, USA). These acquisitions were performed under stable conditions, specifically at room temperature to maintain consistency and reproducibility. In terms of the imaging dynamics, the frame rate was maintained between 0.02 and 0.04 s per frame, translating to an average capture rate of approximately 40 frames per second. Every image was captured using the same exposure time to ensure that no variance in image quality or intensity. Post-acquisition, video files were initially saved in the.avi format. To enhance compatibility and editing capabilities, these files

were subsequently converted to uncompressed.avi formats using VirtualDub software, (https://www.virtualdub.org). For further image processing and analysis, the files also converted to.tiff/.tif format using ImageJ software, 1.53p version (https://imagej.nih.gov/ij). ROIs were confined using the ROI manager in ImageJ. This precision allowed for comprehensive analysis of multiple region of organoids using the plugin function available in ImageJ. Specifically, we employed the Time-lapse video plugin, which facilitate our analysis by providing detail insight into the intensity versus time pattern of the calcium imaging. Only organoids exhibiting baseline calcium transients were chosen for imaging experiments, thereby minimizing potential discrepancies and enhancing the reliability of our results.

Ion delivery using the bioelectronic ion pump

The bioelectronic ion pump was integrated with organoids placed in a six-well plate for ion delivery experiments. Each well has a diameter of 34.8 mm, a total volume of 16.8 mL, and a working volume of 3 mL. After incubation, brain organoids with dimensions of 2.3–2.6 mm were transferred to one of the wells containing BrainPhys Imaging Optimized Medium supplemented with N-2 Supplement, Chemically Defined Lipid Concentrate, and B-27 Supplement with 4μM Fluo-8 a.m. for calcium imaging experiments. After a 30-min incubation at 5% CO2 and 37°C, we placed the plate in the microscope with the ion pump fitted using a 3D printed adaptor. The capillary from the pump (7 mm) with an outlet delivering K+ and GABA was positioned approximately <1 mm from the region of interest (ROI) on the organoid. We confirmed this placement using an inverted fluorescence microscope (EVOS M7000 Imaging System, Invitrogen, USA) by placing the organoid in the center of the field of view and then began calcium imaging. Once we identified a region with at least three ROIs showing spontaneous activity, we started our experiments. We recorded 1 min of spontaneous activity and then proceeded to record activity at the ROIs while the ion pump was delivering the ions of interest. To perform the media exchange according to our stimulation paradigm, we connected the inlet and outlet to flow solution pre-warmed media at a rate of 3 mL/min using a VWR minipump variable flow (Model 3385). After delivery, we washed out the ions for 60 s using a flow rate of 3 mL/min.

QUANTIFICATION AND STATISTICAL ANALYSIS

Strategies for quantitatively assaying ion concentrations and acquisition/processing of imaging data are described in the sections above. Information about plotting uncertainty in Ca^{+} fluorescence signal, ion pump currents, and numbers/types of replicates are provided in the relevant figure legends.

Cell Reports Methods, Volume *4*

Supplemental information

Modulation of neuronal activity in cortical organoids with bioelectronic delivery of ions and neurotransmitters

Yunjeong Park, Sebastian Hernandez, Cristian O. Hernandez, Hunter E. Schweiger, Houpu Li, Kateryna Voitiuk, Harika Dechiraju, Nico Hawthorne, Elana M. Muzzy, John A. Selberg, Frederika N. Sullivan, Roberto Urcuyo, Sofie R. Salama, Elham Aslankoohi, Heather J. Knight, Mircea Teodorescu, Mohammed A. Mostajo-Radji, and Marco Rolandi

Supplemental information

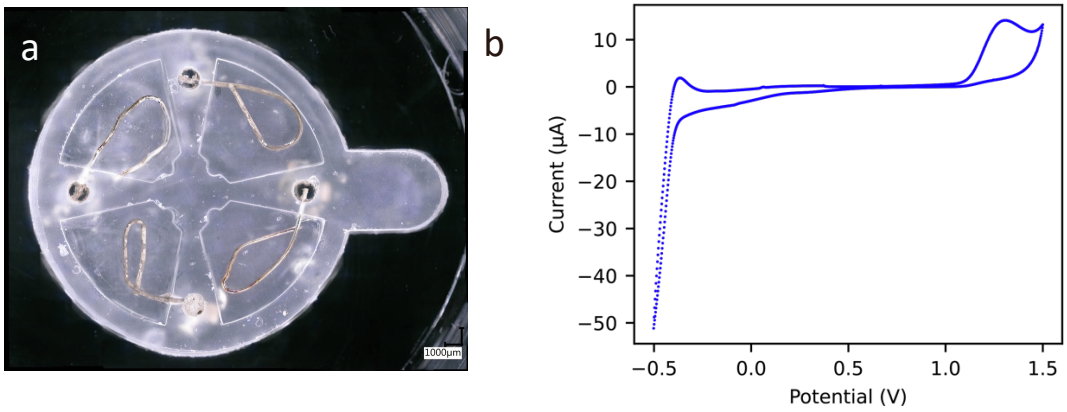

Figure S1. a) Placement of electrodes in the reservoirs related to Figure 1. Electrodes made of 250 mm diameter approximately 7 mm long Ag were embedded within the PDMS reservoirs and twisted to maximize the surface area. Each reservoir was subsequently filled with either KCl or GABA solution. (Scale bar: 1 mm). **b)** Cyclic voltammetry scan of 0.1 M GABA-HCl solution. WE and RE are 0.1 mm diameter Pt. RE was a standard Ag/AgCl reference in a saturated KCl salt bridge. The oxidation reaction of GABA starts to happen at a potential above 1.1 V vs Ag/AgCl.

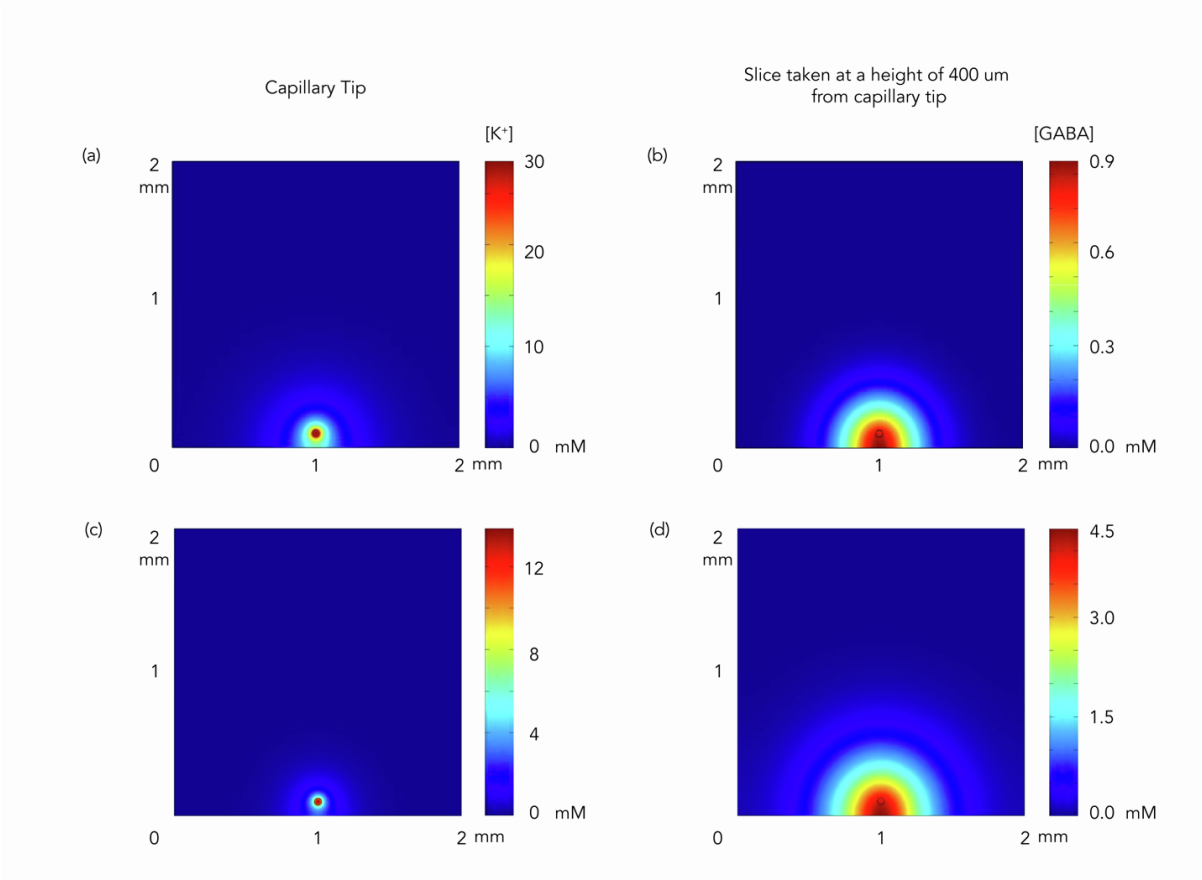

Figure S2. **Simulation results illustrating ion diffusion related to Figure 3.** (a) Concentration dynamics at the K^+ capillary tip. (b) Concentration of K^+ at a 400 µm slice distance from the capillary tip. (c) Concentration dynamics at the GABA capillary tip. (d) Concentration of GABA at a 400 µm slice distance from the capillary tip. The model for the simulation is based on basic diffusion dynamics, without accounting for continuous ion delivery.

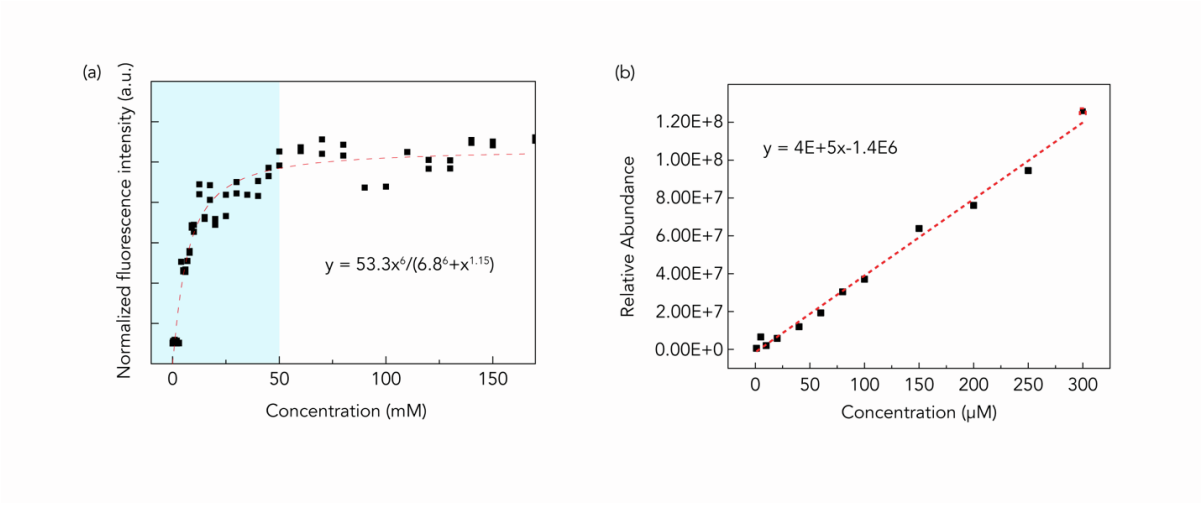

Figure S3. Calibration data for K^+ and GABA concentrations related to Figure 3 and 4. (a) Calibration data showing the relationship between K^+ concentration and fluorescence intensity. (b) Calibration data displaying the relationship between GABA concentration and liquid chromatography (LC) measurements of relative abundance.

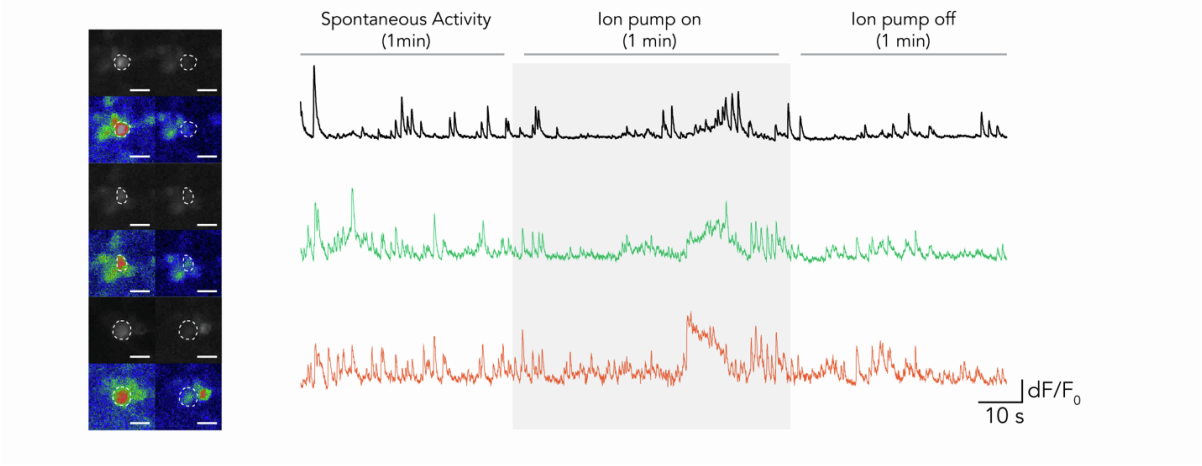

Figure S4. Control experiment using DI water in the reservoir Related to Figure 3 and 4. Sequential neural activity in cortical organoids using DI water filled ion pump (left) Representative image of organoids. (right) The changes in fluorescence intensity over time, show the dynamic changes in neuronal activity. (Scale bar: 10 μm)

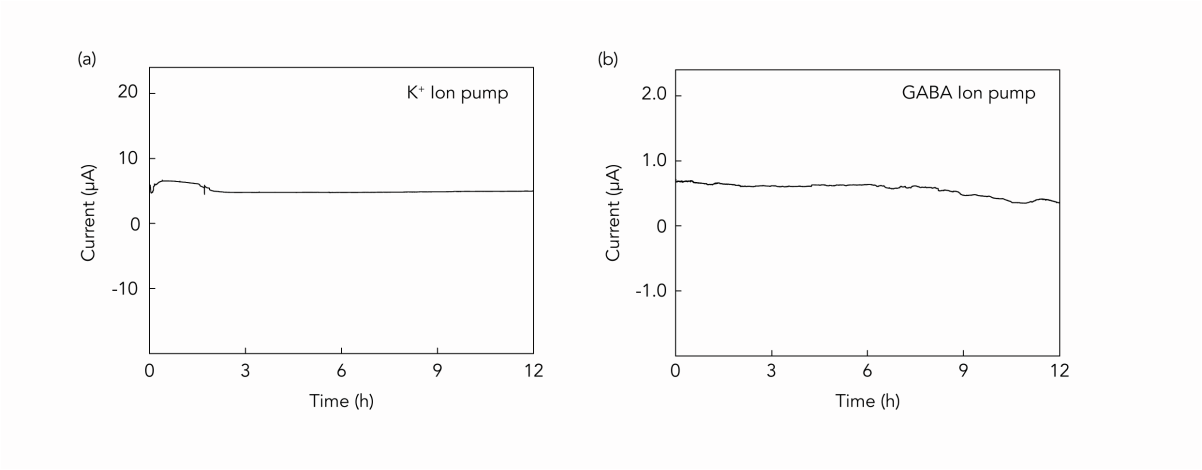

Figure S5. **Evaluation of the stability of the device over extended periods of operation related to Figure 5.** (a) K^+ ion pump with V_{K+}= 1V and V_{GABA}= 1V. (b) GABA ion pump.